BIOLOGY OF REPRODUCTION **83,** 774–782 (2010)
Published online before print 14 July 2010.
DOI 10.1095/biolreprod.110.085175

Insulin-Like 3 Exposure of the Fetal Rat Gubernaculum Modulates Expression of Genes Involved in Neural Pathways[1]

Kamin J. Johnson,[2] Alan K. Robbins, Yanping Wang, Suzanne M. McCahan, Job K. Chacko, and Julia S. Barthold

Nemours Biomedical Research, Alfred I. duPont Hospital for Children, Wilmington, Delaware

ABSTRACT

Insulin-like 3 (INSL3) signaling directs fetal gubernacular development and testis descent, but the actions of INSL3 in the gubernaculum are poorly understood. Using microarray gene expression profiling of fetal male rat gubernaculum explants exposed to 10 or 100 nM INSL3, significant changes in expression were identified for approximately 900 genes. Several of the genes showing the largest inductions regulate neuronal development or activity, including *Pnoc* (34-fold), *Nptx2* (9-fold), *Nfasc* (4-fold), *Gfra3* (3-fold), *Unc5d* (3-fold), and *Crlf1* (3-fold). Bioinformatics analysis revealed BMP and WNT signaling pathways and several gene ontologies related to neurogenesis were altered by INSL3. Promoter response elements significantly enriched in the INSL3-regulated gene list included consensus sequences for MYB, REL, ATF2, and TEF transcription factors. Comparing in vivo gene expression profiles of male and female rat fetal gubernaculum showed expression of the *Bmp*, *Wnt*, and neurodevelopmental genes induced by INSL3 was higher in males. Using quantitative RT-PCR, the microarray data were confirmed, and the induction of *Bmp3*, *Chrdl2*, *Crlf1*, *Nptx2*, *Pnoc*, *Wnt4*, and *Wnt5a* mRNA levels were examined over a range of INSL3 concentrations (0.1–100 nM) in male and female gubernaculum. In both sexes, an increasing gene expression response was observed between 0.1 and 10 nM INSL3. These data suggest that INSL3 signaling in the fetal gubernaculum induces morphogenetic programs, including BMP and WNT signaling, and support other rodent data suggesting a role for these pathways in development of the gubernaculum.

cryptorchidism, gene expression profiling, gubernaculum, hormone actions, insulin-like 3, male reproduction, male reproductive tract, mechanisms of hormone action, neuron

INTRODUCTION

During mammalian development, the testis normally descends into the scrotum, but the human condition of undescended testis (cryptorchidism) is relatively frequent, occurring in 2–4% of male births [1]. If the testis fails to descend, spermatogenesis is disrupted, leading to subfertility. Cryptorchidism is also associated with other conditions of male reproductive maldevelopment, including hypospadias and testis cancer. The causes of human cryptorchidism are not well understood, but roles for genetic polymorphisms and environmental chemical exposures are postulated [2].

In mammals, testis descent occurs during both fetal and neonatal life and is controlled by testis-produced hormones (insulin-like 3 [INSL3] and androgen) that drive male-specific development of a ligament called the gubernaculum [3, 4]. At its cranial pole, the gubernaculum is attached to the testis/epididymal complex and enlarges in response to testis hormones, creating a space within the inguinal canal that facilitates testis descent. In male fetal rats, the bulk of the fetal gubernaculum, called the bulb, is composed of a core of mesenchymal cells surrounded by striated muscle that is continuous with the abdominal wall musculature and innervated by the genitofemoral nerve. The gubernaculum develops in both sexes and is histologically similar until Gestational Day (GD) 16 in the rat fetus but enlarges in males only during GDs 16–20 [5–8]. Exposure of GD 17 rat gubernacula to INSL3 and androgen in vitro stimulates cellular proliferation and development of both mesenchymal and muscle layers within the gubernaculum [7, 9]. The only receptor for INSL3 is a G protein-coupled receptor called relaxin/insulin-like peptide family receptor 2 (RXFP2) [10], and *Rxfp2* mRNA and protein expression is detected in the muscle layer of the fetal gubernaculum [11]. In mice with an *Insl3* or *Rxfp2* null mutation, the male gubernaculum fails to enlarge normally, and testes remain within the abdominal cavity [12–14]. Conversely, transgenic overexpression of INSL3 in female mice causes abdominal translocation of the fetal ovary and male-like development of the gubernacular bulb [15, 16]. These data show that INSL3-dependent signaling via RXFP2 within the fetal gubernaculum critically controls the initial phase of testis descent.

The only reported effects of INSL3 signaling in the gubernaculum are production of the second-messenger cAMP, histological changes in muscle and mesenchyme, and tissue enlargement, caused in part by increased cell proliferation [7, 9, 16]. The goal of the present study was to identify downstream pathways that are activated by INSL3-RXFP2 signaling in the gubernaculum that may provide insight regarding genetic factors contributing to cryptorchidism. We hypothesized that INSL3 would induce a morphogenetic program in the fetal gubernaculum based upon changes in gene expression, and this hypothesis was tested by examining the gene expression profile of the male and female fetal rat gubernacular bulb following in vitro exposure to INSL3.

MATERIALS AND METHODS

Animals

Breeding colonies of Long-Evans rats were maintained at the Alfred I. duPont Hospital for Children in a facility accredited by the Association for Assessment and Accreditation of Laboratory Animal Care International, and animal care and use was approved by the Institutional Animal Care and Use Committee of the hospital. Rats were provided food (LabDiet Rat Chow 5021;

[1]Supported by National Institutes of Health grant P20RR020173 (J.S.B.).
[2]Correspondence: Nemours Biomedical Research, Alfred I. duPont Hospital for Children, 1600 Rockland Rd., Wilmington, DE 19803. FAX: 302 651 6782; e-mail: johnson@medsci.udel.edu

Received: 5 April 2010.
First decision: 28 April 2010.
Accepted: 28 June 2010.

eISSN: 1529-7268 http://www.biolreprod.org
ISSN: 0006-3363

PMI Nutrition International) and water ad libitum and housed in polycarbonate cages with pine-shaving bedding in a room with a 12L:12D photoperiod and controlled temperature (70 ± 2°C) and humidity (35–70%). Following overnight cohabitation, females fertilized by males were identified by sperm in vaginal lavage fluid. When sperm were detected, this day was designated GD 0. On GD 17, between 1200 and 1500 h, dams were euthanized by carbon dioxide asphyxiation and pups by decapitation.

Gubernaculum Tissue Culture and INSL3 Exposure

The culture system was modeled after that described by Emmen et al. [7]. Immediately after microdissection, two GD 17 gubernacular bulbs per biological replicate were cultured on a Millicell CM membrane (catalog no. PICM03050; Millipore Corp.) in six-well polystyrene culture plates (catalog no. 3506; Corning, Inc.) containing 1 ml of medium per well. All medium reagents were obtained from Invitrogen Corp. and included Dulbecco modified Eagle medium/Ham F12 (catalog no. 21041–025), 2% charcoal stripped fetal bovine serum (catalog no. 12676–011), 1× insulin-transferrin-selenium-X supplement (catalog no. 51500–056), and 1× antibiotic-antimycotic (catalog no. 15240–096). Cultures were maintained at 37°C in a humidified chamber with 5% carbon dioxide. For female gubernacula, tissue was incubated immediately with medium containing no hormone (control) or mouse INSL3 (catalog no. 035–43; Phoenix Pharmaceuticals, Inc.). This recombinant mouse INSL3 has been shown to stimulate cAMP production in cells via RXFP2 [10]. Because GD 17 male rat gubernacula have been exposed to INSL3 in vivo for approximately 2 days [11], male gubernacula were cultured for 24 h in medium containing no INSL3 to reduce any preexisting, INSL3-dependent gene expression. Gubernacula were then cultured for 24 h with either basal or INSL3-containing medium. The INSL3 concentrations employed (0.1–100 nM) bracketed the dissociation constant of INSL3 for its receptor (RXFP2) [17–19] and the estimated minimum in vivo exposure of the fetal gubernaculum based on serum INSL3 levels at GD 17 of approximately 0.5–1 nM (unpublished observations). Local levels of INSL3 likely are higher based on experimental data showing that unilateral castration of rabbit fetuses inhibits ipsilateral, but not contralateral, development of the gubernaculum [20].

Microarrays

Group (biological replicate) sizes for the microarrays were six control replicates, five 10 nM INSL3 replicates, and six 100 nM INSL3 replicates. These two concentrations were chosen because they elicited maximal stimulation of cAMP production in primary gubernacular cells and *Rxfp2*-transfected cells [17]. Total RNA was isolated using an RNeasy Micro Kit (Qiagen), with genomic DNA digested on the column. RNA quality was verified with an Agilent 2100 Bioanalyzer, and RNA Integrity Numbers of greater than nine were obtained. Next, 150 ng of total RNA were labeled using a GeneChip 3′ IVT Express Kit (Affymetrix, Inc.). Using a GeneChip Scanner 3000 7G System (Affymetrix, Inc.), 15 μg of biotin-labeled cRNA were hybridized to GeneChip Rat Genome 230 2.0 microarrays (Affymetrix, Inc.) containing approximately 31 000 probesets. After washing and staining, microarrays were scanned to obtain raw signal intensities for each probe, and these were background-corrected, normalized, and summarized using Guanine Cytosine Robust Multiarray Analysis and the affylmGUI Bioconductor package within R (http://www.bioconductor.org/). Microarray data were deposited in the Gene Expression Omnibus of the National Center for Biotechnology Information (NCBI; www.ncbi.nlm.nih.gov/geo/) and assigned accession number GSE19658. Principal component analysis was performed on the normalized expression data and showed that the INSL3 exposure replicates grouped together with the exception of two replicates in the 10 nM INSL3 group (data not shown). Compared to all the other samples, these two samples also had low cRNA yields (data not shown). Therefore, these two replicates were excluded from further analysis.

Gene profiling methodology for the GD 17.5 male and female gubernacula comparison used GeneChip RAE230A microarrays (Affymetrix, Inc.) containing approximately 16 000 probesets. Raw data acquisition and samples for these arrays have been described previously [21].

Quantitative RT-PCR

Gubernaculum starting material for these experiments was distinct from gubernacula used for microarray analysis. Total RNA purification, cDNA generation, Taqman-based PCR, and data analysis using the delta-delta threshold cycle method were performed as described previously [21]. Expression of target genes was normalized to *Gapdh* expression and quantified relative to expression in a fetal rat embryo total RNA preparation (catalog no. AM7928; Applied Biosystems/Ambion). Prevalidated Taqman assays (Applied Biosystems, Inc.) were as follows: *Bmp3*, Rn00567346_m1; *Chrdl2*, Rn01510694_m1; *Crlf1*, Rn01419973_m1; *Nptx2*, Rn01756377_m1; *Pnoc*, Rn00564560_m1; *Wnt4*, Rn00584577_m1; *Wnt5a*, Rn00575260_m1; and *Gapdh*, Rn99999916_s1.

Microarray and Quantitative RT-PCR Statistical Analysis

Before statistical analysis of the microarray data, an expression filter was applied to exclude probesets showing a log2 expression value of less than 3.5 in all replicates of at least one group. Using the LIMMA package in Bioconductor (http://www.bioconductor.org/), probesets with a significant expression change after INSL3 exposure were identified using a linear model approach with false-discovery rate (FDR) correction. Probesets with an FDR-corrected *P* value of less than 0.05 were considered to be significantly changed.

Significance testing of quantitative RT-PCR (qRT-PCR) data was performed with GraphPad Prism 5.0 software and used one-way ANOVA and Dunnett post-hoc tests. *P* values of less than 0.05 were deemed to be significant.

Bioinformatics

Bioinformatics pathway analysis was performed on lists of genes (i.e., probesets) with a significant change in expression after INSL3 exposure. To be included in the analysis, a gene had to have an FDR-corrected *P* value of less than 0.05 in both the 10 and 100 nM exposure groups. Various gene lists were analyzed: 1) all significant probesets, 2) significant probesets with an expression fold-change greater than or equal to an absolute value of 1.5, and 3) significant probesets with an expression fold-change greater than or equal to an absolute value of 2. Pathway analysis was conducted using both Ingenuity Pathway Analysis (IPA: version 8.0; Ingenuity Systems, Inc.) and the Database for Annotation, Visualization, and Integrated Discovery (DAVID; version 2008) [22]. Both IPA and DAVID provide complementary pathway analysis: IPA uses a proprietary knowledge base, whereas DAVID considers ontologies from the Gene Ontology (GO) project and pathways from the Kyoto Encyclopedia of Genes and Genomes (KEGG). Before importing gene lists into IPA, probesets not annotated to a Human Genome Organization gene symbol by Affymetrix were annotated by performing a Basic Local Alignment Search Tool search with public domain software provided by the National Center for Biotechnology Information and using the probeset target sequence. Gene symbols were assigned to a probeset when a mammalian gene with a RefSeq mRNA accession had an alignment score to the target sequence of greater than or equal to 200. Using gene symbols as identifiers, gene lists were imported into IPA and DAVID [22]. Within IPA, statistically significant molecular pathways enriched in the gene list were determined from the IPA library of canonical pathways, and an FDR-corrected Fisher exact test *P* value of less than 0.05 was considered to be significant. For DAVID analysis, the 16 504 probesets expressed in control and/or hormone-exposed gubernacula were used as the gene population background, annotations were limited to *Rattus norvegicus*, default analysis parameters were employed, and GO annotation terms and KEGG pathways with a Benjamini-corrected Fisher exact test *P* value of less than 0.05 were considered to be significant.

Promoters of differentially expressed genes (identified for both 10 and 100 nM INSL3) were analyzed for enrichment of transcription factor binding sites using Promoter Analysis and Interaction Network (PAINT; v3.9; www.dbi.tju.edu/dbi/tools/paint) [23]. Affymetrix probeset IDs were converted to mouse NCBI Gene IDs using NetAffx and NCBI Homologene databases. DNA sequences for 665 Gene IDs were in the PAINT database. These sequences, which included 2 kb upstream of each transcription start site, were examined for transcription binding sites defined in the Transfac 7.0 Public 2005 database using PAINT v3.9. Binding site enrichment was determined by comparison to all mouse promoters in the PAINT database, and an FDR-corrected *P* value of 0.1 or less was considered to be significant.

RESULTS

INSL3-Dependent Microarray Gene Profiling and Functional Pathway Analysis

Gene expression microarray analysis was used to identify mRNA transcripts in fetal male rat gubernaculum modulated by exposure to INSL3. Male GD 17 gubernacular bulb cultures exposed to 10 or 100 nM INSL3 for 24 h were examined. Of the approximately 31 000 queried probesets, 3482 displayed significantly altered expression in response to at least one INSL3 concentration (Supplemental Tables S1 and S2; all

TABLE 1. Neurogenesis and synaptic transmission genes upregulated at least 2-fold by INSL3.

Gene symbol	Gene name	Fold change	
		10 nM INSL3	100 nM INSL3
Pnoc	Prepronociceptin	34.1	38.5
Gda	Guanine deaminase	28.8	67.7
Pcdh8	Protocadherin 8	17.3	33.2
Nptx2	Neuronal pentraxin 2	9.7	9.2
Ctnnd2	Catenin delta 2	4.4	2.9
Slc6a1	Solute carrier family 6, member 1	4.2	3.1
Unc5d	Unc-5 homolog D	3.7	3
Nfasc	Neurofascin	3.5	4
Homer2	Homer homolog 2	3.1	3.4
Adra2a	Adrenergic receptor, alpha2a	3	3.4
Crlf1	Cytokine receptor-like factor 1	2.8	2.7
Gfra3	GDNF family receptor alpha 3	2.9	3.5
Glrb	Glycine receptor, beta subunit	2.7	2.5
Dok5	Docking protein 5	2.7	2.2
Vldlr	Very low density liporprotein receptor	2.6	2.6
Ngfr	Nerve growth factor receptor	2.4	2.6
Sema3g	Semaphorin 3g	2.3	2.7

Supplemental Data are available online at www.biolreprod.org). Similar numbers of probesets with significant expression changes were observed at 10 or 100 nM INSL3 (2167 and 2302 probesets, respectively). Only 20 probesets were significantly different between 10 and 100 nM INSL3 exposures, and these differences were generally in magnitude of expression, not in direction of change. Compared to 100 nM INSL3, the 10 nM INSL3 gene list contained nearly twice as many genes with a 1.5-fold or greater expression decrease, but most (~67%) of these decreased genes were not significantly altered by 100 nM INSL3. Using qRT-PCR analysis of a separate series of INSL3-exposed tissue, we failed to confirm the reduced microarray expression of five genes (*Axin2*, *Ccnd2*, *Gsk3b*, *Lrp6*, and *Sfrp1*) that were identified only in the 10 nM INSL3 group. However, we were able to corroborate the expression change of all seven analyzed genes significantly altered by both 10 and 100 nM INSL3 (see below). Therefore, downstream bioinformatics analyses of the microarray data were limited to those genes with significant changes in expression after both 10 and 100 nM INSL3 exposure. This list contained a total of 989 probesets, representing approximately 900 unique genes (Supplemental Table S2). Increased expression was observed for 714 probesets, and of these, 180 were upregulated at least 2-fold. The robustness of this gene list was exemplified by an excellent correlation of the direction of expression change observed between 10 and 100 nM exposures: All 989 probesets showed the same direction of expression change at both 10 and 100 nM INSL3.

Within the INSL3 upregulated gene list, *Pnoc* (encoding the secreted neuropeptide nociceptin) displayed the greatest INSL3-induced expression change (34-fold by 10 nM INSL3), and a gene encoding a prohormone convertase known to process prepronociceptin (*Pcsk2*) also was highly upregulated (9-fold by 10 nM INSL3). In gubernacular cells, INSL3 binding to RXFP2 increases production of cAMP [18], and in other tissues, cAMP elevates the *Icer* form of *Crem* [24] and phosphodiesterase mRNA levels [25]. Consistent with cAMP production in our culture model, mRNA levels of *Crem* and three cAMP phosphodiesterases (*Pde10a*, *Pde8a*, and *Pde4d*) were upregulated between 2- and 13-fold. A number of genes with large fold-change increases are involved in neurogenesis or modulation of synaptic transmission, including several secreted ligands and receptors for secreted ligands (Table 1).

Pathway analysis of the INSL3 microarray data revealed molecular signaling and cellular differentiation programs potentially downstream of INSL3 signaling in the gubernaculum. The INSL3-responsive gene list was examined with pathway analysis software using all significantly changed genes or gene subgroups with a 1.5- or 2-fold expression change. IPA canonical signaling pathways significantly enriched in the gene lists are shown in Table 2, and genes with significant expression changes in each pathway and images of the pathways can be found in Supplemental Table S3 and Figures S1–S3. Many of the observed pathways were detected because they incorporated Wnt and/or Bmp signaling. On their own, Wnt/β-catenin and Bmp canonical signaling pathways were significantly changed by INSL3 exposure. Within the Wnt and Bmp pathways, mRNAs of several ligands, including *Wnt2*, *Wnt4*, *Wnt5a*, *Wnt9a*, and *Wnt16* and *Bmp1*, *Bmp2*, *Bmp3*, *Bmp5*, and *Bmp7*, were upregulated. One of the most highly induced genes encodes a BMP antagonist (*Chrdl2*; increased 13-fold by INSL3). When only genes with a relatively high expression fold-change of greater than 1.5 or 2 are included in the analysis, the cAMP-mediated signaling and BMP signaling pathways became statistically significant. The same pathways were called significant only if genes with increased expression were used in the analysis, and only the WNT/β-catenin canonical pathway was detected when genes with decreased expression were examined (data not shown). Therefore, genes induced by INSL3 were largely responsible for all IPA canonical pathway significance calls.

In addition to IPA, we extracted biological meaning from the microarray gene expression data using DAVID and PAINT. Table 3 shows selected statistically significant GO annotation terms and KEGG pathways derived from the INSL3-regulated gene list using DAVID. All GO terms and KEGG pathways with a corrected *P* value of less than 0.05 and associated genes are found in Supplemental Table S4. Prominent within the list of annotation terms were those related to neurodevelopment, including the higher-level ontology terms nervous system development and neurogenesis as well as subcategories such as neuron differentiation, generation of neurons, and axonal guidance. Another potential functional role of INSL3 may be cholesterologenesis, because genes in the GO term sterol metabolic process were significantly modulated by INSL3; several of these genes were induced between 1.5- and 2-fold and are involved in cholesterol biogenesis (*Cyp51*, *Hmgcr*,

TABLE 2. Pathway analysis of INSL3-responsive genes using Ingenuity Pathways Analysis (IPA).[a]

IPA canonical pathway	All genes[b]	1.5-Fold genes[c]	2-Fold genes[d]
Human embryonic stem cell pluripotency	7E-07	5E-05	0.042
Basal cell carcinoma signaling	1E-06	3E-05	0.022
WNT/β-catenin signaling	9E-06	0.001	0.045
Role of osteoblasts, osteoclasts, and chondrocytes in rheumatoid arthritis	9E-06	0.001	0.043
Axonal guidance signaling	1E-04	1E-04	0.012
Colorectal cancer metastasis signaling	1E-04	0.001	0.022
Role of nanog in mammalian embryonic stem cell pluripotency	1E-04	0.017	NS
Factors promoting cardiogenesis in vertebrates	6E-04	0.004	NS
Ovarian cancer signaling	9E-04	0.005	NS
Tight junction signaling	9E-04	NS	0.045
Role of macrophages, fibroblasts, and endothelium in rheumatoid arthritis	0.005	NS	NS
Inositol metabolism	0.006	NS	NS
Hepatic fibrosis/hepatic stellate cell activation	0.006	0.01	0.026
Leukocyte extravasation signaling	0.049	0.01	NS
HGF signaling	0.049	NS	NS
BMP signaling	NS	0.049	NS
cAMP-mediated signaling	NS	0.049	0.012

[a] Values in the table are significance measures (Benjamini-Hochberg-corrected *P* values) of each pathway; NS, not significant.
[b] Analyzed gene list contained all significant genes.
[c] Analyzed gene list contained all significant genes with a 10 nM INSL3 expression change ≥1.5-fold.
[d] Analyzed gene list contained all significant genes with a 10 nM INSL3 expression change ≥2-fold.

Idi1, *Lss*, *Sc4mol*, *Sc5dl*, *Srebf1*, and *Srebf2*). Like the IPA analysis, the significant KEGG pathway basal cell carcinoma consisting of WNT pathway factors was enriched significantly. GO terms related to subcellular locations that were over-represented included extracellular space and plasma membrane. The subset of gubernaculum genes induced by INSL3 produced similar significantly enriched GO terms through DAVID analysis (data not shown). Using PAINT, transcription factor consensus sequences over-represented within promoters of genes modulated by INSL3 were determined. When all INSL3-responsive genes, only upregulated genes, or only downregulated genes were analyzed, PAINT revealed that consensus binding sequences for four transcription factors (ATF2, TEF, REL, and MYB) were significantly enriched in INSL3-modulated genes (Table 4 and Supplemental Table S5). The number of genes with identified promoter consensus sites for ATF2, TEF, REL, and MYB were 7, 8, 83, and 83, respectively. By microarray analysis, *Tef* expression was increased after INSL3 exposure.

TABLE 3. Selected DAVID gene functional classifications of INSL3 altered gene list.[a]

Classification	All genes[b]	1.5-Fold genes[c]	2-Fold genes[d]
GO biological process terms			
Nervous system development (GO:0007417)	3.4E-6	2.5E-05	NS
Neurogenesis (GO:0022008)	2.2E-4	0.005	NS
Neuron differentiation (GO:0030182)	0.006	0.007	NS
Neuron projection morphogenesis (GO:0048812)	0.006	0.01	NS
G protein-coupled receptor protein signaling pathway (GO:0007186)	0.01	0.007	0.02
Generation of neurons (GO:0048699)	0.011	0.037	NS
Response to peptide hormone stimulus (GO:0043434)	0.016	NS	NS
Neuron development (GO:0031175)	0.016	0.032	NS
Negative regulation of apoptosis (GO:0043066)	0.025	NS	NS
Mesenchyme development (GO:0060485)	0.029	0.029	NS
Regulation of cell proliferation (GO:0042127)	0.036	NS	NS
Sterol metabolic process (GO:0016125)	0.038	0.049	NS
Axon guidance (GO:0007411)	NS	0.021	NS
cAMP-mediated signaling (GO:0019933)	NS	0.049	NS
GO cellular component terms			
Extracellular space (GO:0005615)	0.003	0.009	0.026
Plasma membrane (GO:0005886)	0.003	0.001	0.002
KEGG pathways			
Basal cell carcinoma (rno05217)	0.04	0.029	NS
Steroid biosynthesis (rno00100)	NS	0.028	NS
Neuroactive ligand-receptor interaction (rno04080)	NS	NS	0.037

[a] Values in the table are significance measures (Benjamini-corrected *P* values) of each GO term determined using the database for Annotation, Visualization, and Integrated Discovery (DAVID; http://david.abcc.ncifcrf.gov/home.jsp); NS, not significant.
[b] Analyzed gene list contained all significant genes.
[c] Analyzed gene list contained all significant genes with a 10 nM INSL3 expression change of ≥1.5-fold.
[d] Analyzed gene list contained all significant genes with a 10 nM INSL3 expression change of ≥2-fold.

TABLE 4. Transcription factor binding site analysis using PAINT of INSL3-responsive genes.[a]

TF/TFBS[b]	Consensus sequence	TF gene symbol	All genes[c]	Increased genes[d]	Decreased genes[e]
VBP/V$VBP_01	RTTACRTMAK	*Tef*	0.078	0.006	NS
CRE-BP1/V$CREBP1_01	TTACGTAA	*Atf2*	NS	0.065	NS
c-Rel/V$CREL_01	SGGRNTTTCC	*Rel*	NS	0.085	NS
v-Myb/V$VMYB_01	GCCAACTGAC	*Myb*	0.083	NS	NS

[a] Numerical values in the table are significance measures (false discovery rate-corrected *P* values) of each transcription factor binding site element within the gene list examined as determined using Promoter Analysis and Interaction Network Toolset (PAINT; www.dbi.tju.edu/dbi/tools/paint/); NS, not significant ($P \geq 0.1$).
[b] TF, transcription factor; TFBS, transcription factor binding site.
[c] *P* value when all significant INSL3-reponsive genes were analyzed.
[d] *P* value when genes increased significantly by INSL3 were analyzed.
[e] *P* value when genes decreased significantly by INSL3 were analyzed.

Because high INSL3 levels are found in male compared to female fetuses, we predicted that many of the genes modulated by INSL3 in the gubernaculum culture model would show significant expression differences in vivo between male and female gubernacula. Furthermore, a large number of genes increased by INSL3 in culture should show increased expression in male compared to female gubernacula. To examine these predictions, in vivo microarray gene expression data from GD 17.5 male and female gubernacula (Supplemental Table S6) were compared with genes meeting two criteria from the gubernaculum INSL3 exposure experiment: 1) a significant expression change after both 10 and 100 nM INSL3 exposure, and 2) a 2-fold or greater change following 10 nM INSL3 exposure. Because of the different microarray chips used in each experiment, only those probesets meeting these two criteria and present on both microarrays were compared. Of 108 probesets increased by INSL3 and tested in both experiments, seven showed higher expression in female gubernacula, 51 were not significantly different between male and female gubernaculum, and nearly half (n = 50) displayed higher expression in male gubernaculum (Supplemental Table S7). Similar results were observed for genes decreased by INSL3 exposure. Of 35 probesets decreased by INSL3 exposure and also examined in male and female gubernacula in vivo, nine were not significantly different between male and female gubernaculum, five had higher expression in male gubernaculum, and more than half (n = 21) displayed reduced expression in male gubernaculum. Thus, fetal gubernaculum genes responsive to INSL3 exposure in vitro generally exhibit similar differential expression between male and female fetal gubernaculum in vivo.

Microarray Data Confirmation and Concentration Response of INSL3-Induced Gene Expression

To confirm the INSL3 microarray data and examine the timing and INSL3 concentration response of gene expression in fetal gubernaculum, a set of rat gubernacula not used in the microarray experiments were exposed to INSL3, and the expression of seven genes was analyzed by qRT-PCR. These seven genes were chosen because they displayed increased expression in male compared to female gubernaculum and are involved in Bmp signaling, Wnt signaling, or neurodevelopmental pathways identified via bioinformatics analyses. Using the same 24-h exposure model as for the microarray experiment, male gubernacula were incubated with INSL3 concentrations ranging from 0.1 to 100 nM. Overall, excellent concordance was found between the microarray and qRT-PCR

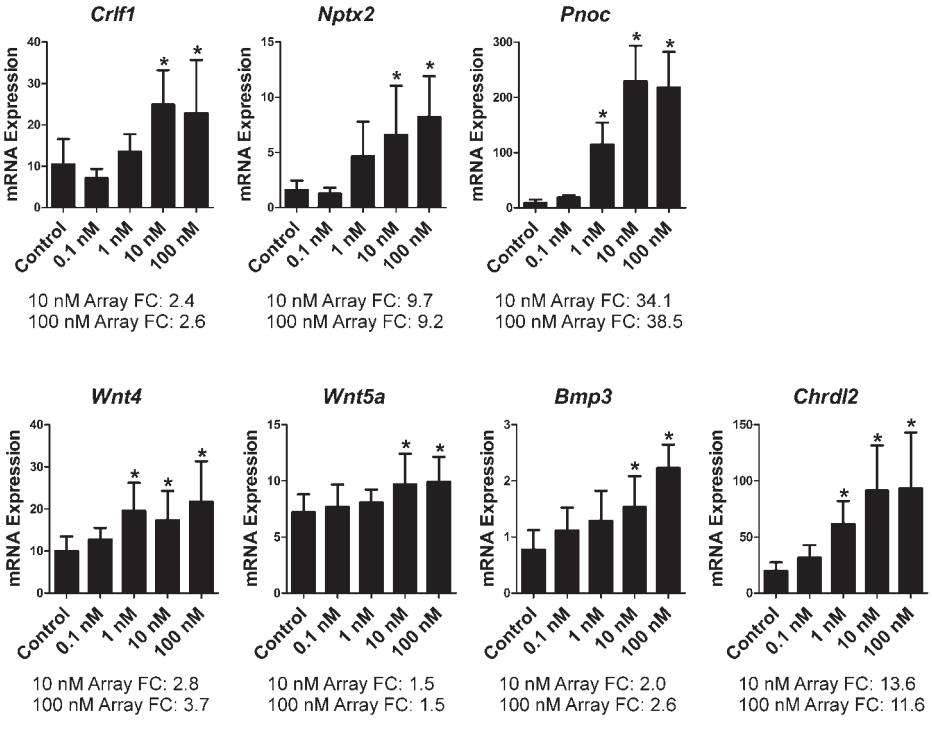

FIG. 1. After incubation for 24 h in the presence of INSL3 concentrations ranging from 0 (control) to 100 nM, male fetal gubernacular bulb gene expression was examined by Taqman-based qRT-PCR. Each graph shows mRNA levels, with the gene identified above the graph. Below each graph, the fold-change (FC) is given for each gene after 24-h exposure to 10 or 100 nM INSL3 as determined by microarray expression analysis. Data are presented as the mean ± SD (n = 7–11). An asterisk indicates a significant difference from control ($P < 0.05$) as determined by one-way ANOVA and Dunnett post-hoc test.

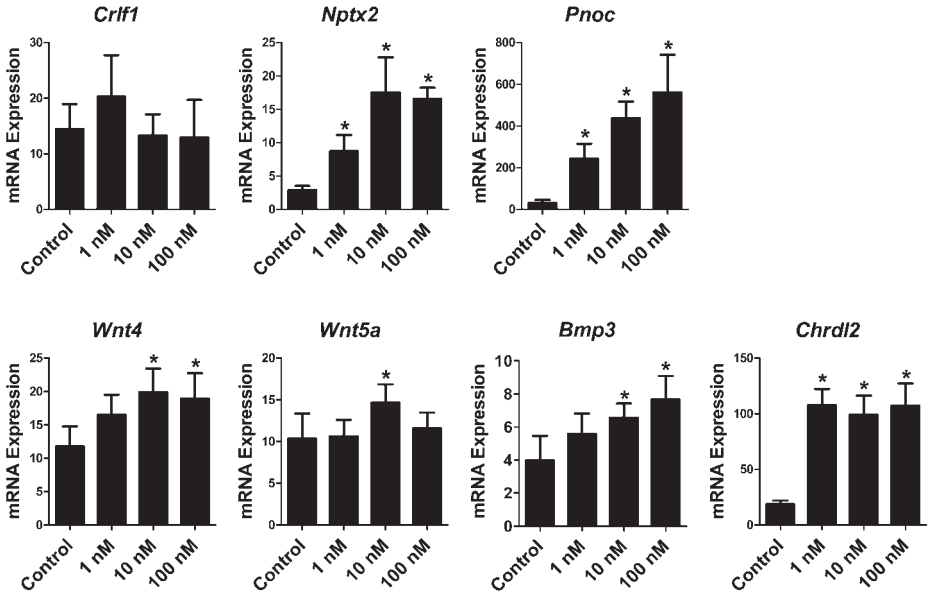

FIG. 2. After incubation for 6 h in the presence of INSL3 concentrations ranging from 0 (control) to 100 nM, male fetal gubernacular bulb gene expression was examined by Taqman-based qRT-PCR. Each graph shows mRNA levels, with the gene identified above the graph. Data are presented as the mean ± SD (n = 5–6). An asterisk indicates a significant difference from control ($P < 0.05$) as determined by one-way ANOVA and Dunnett post-hoc test.

data (Fig. 1). The gene expression response to INSL3 became saturated at 10 nM INSL3 for most genes, although *Wnt4* levels peaked at 1 nM INSL3. Whereas trends were found for increased expression of *Pnoc*, *Wnt4*, *Bmp3*, and *Chrdl2* at 0.1 nM INSL3, the responses did not reach statistical significance using a one-way ANOVA and Dunnett post-hoc test. Using just the control and 0.1 nM values, an unpaired *t*-test produced *P* values of less that 0.05 for these four genes (data not shown).

To determine if a shorter INSL3 exposure modulated gubernaculum gene expression, mRNA levels were examined by qRT-PCR after a 6-h incubation with INSL3 (Fig. 2). In comparing the 6- and 24-h exposures, the responses were gene-specific. After 6 h, no significant expression changes were observed for *Crlf1*, and *Wnt5a* levels were increased at 10 nM, but not at 100 nM, INSL3. For *Wnt4*, *Bmp3*, and *Chrdl2*, the concentration response and level of induction were similar at both time points. Finally, *Nptx2* and *Pnoc* induction levels at 6 h were approximately twice the levels observed at 24 h.

Transgenic expression of INSL3 in fetal female mice causes male-like gubernacular development and transabdominal descent of the ovary [15, 16], suggesting responsiveness of the female gubernaculum to INSL3. Likewise, histological development of the gubernaculum is similar in males and females, but enlargement occurs in males, but not in females, from GD 16 to GD 20 [5–7]. We used female GD 17 gubernacula to provide comparative gene expression data using an anatomically similar organ not previously exposed to INSL3 that is morphologically similar to the male. Overall, female gubernaculum gene expression responses after 24 h of exposure were similar to the responses in males, but for *Bmp3*, *Chrdl2*, and *Wnt4* expression, the female tissue appeared to show increased sensitivity to INSL3 (Fig. 3).

DISCUSSION

Using high content analysis, we examined the gene expression response of cultured fetal rat gubernaculum to INSL3 exposure during its early outgrowth phase. Several results demonstrated the robustness of the microarray data. First, statistical significance and fold-change values were

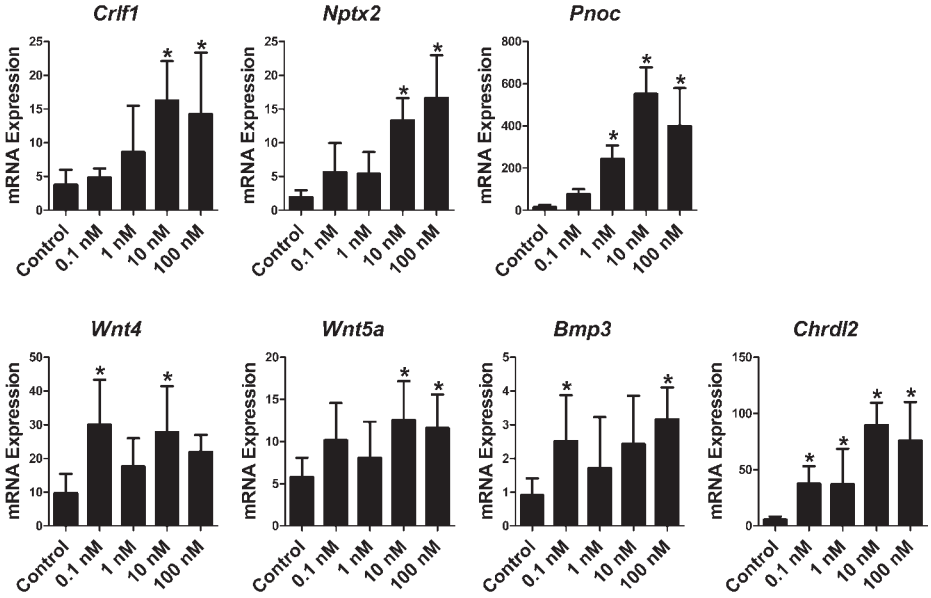

FIG. 3. After incubation for 24 h in the presence of INSL3 concentrations ranging from 0 (control) to 100 nM, female fetal gubernacular bulb gene expression was examined by Taqman-based qRT-PCR. Each graph shows mRNA levels, with the gene identified above the graph. Data are presented as the mean ± SD (n = 6–7). An asterisk indicates a significant difference from control ($P < 0.05$) as determined by one-way ANOVA and Dunnett post-hoc test.

similar for the seven genes examined by both microarray and qRT-PCR. This was observed even though separate biological replicates were used for each technique. Second, data from INSL3-exposed female gubernacula corroborated expression data from male gubernacula. Third, the consensus binding site of a cAMP-responsive transcription factor (ATF2) was over-represented in promoters of genes regulated by INSL3, and genes in the IPA cAMP-mediated signaling canonical pathway were significantly affected by INSL3 exposure. Finally, the microarray gene expression responses following exposures to 10 and 100 nM INSL3 were nearly identical and mirrored INSL3-induced cAMP production at these two concentrations [17–19].

Gubernaculum microarray gene expression and cAMP production data possess similar INSL3 concentration responses. Stimulation of cAMP production downstream of INSL3/RXFP2 binding in *Rxpf2*-transfected cells or primary neonatal gubernaculum cells begins at ligand concentrations of 0.1 nM and becomes maximal at approximately 10 nM [17–19]. Although not true for every gene examined, 0.1 nM INSL3 induced *Bmp3*, *Chrdl2*, *Pnoc*, and *Wnt4* gene expression in male gubernaculum to levels just above control, and expression of most genes became maximal at 10 nM INSL3. This saturation event was observed in both qRT-PCR and microarray expression data. By microarray analysis, mRNA levels of only 20 genes were significantly different between 10 and 100 nM INSL3, even though each INSL3 concentration altered expression of more than 1000 genes. Putting these INSL3 concentration-response data in an in vivo context is difficult, because to our knowledge, no reports of INSL3 protein levels in fetal gubernaculum or serum have been published. However, *Insl3* mRNA levels are high, and INSL3 immunoexpression is readily detected in fetal rat testis [11]. In pubertal male rat serum, INSL3 protein peaked at a concentration of approximately 1 nM [26], and our preliminary data suggest similar concentrations in GD 17 male rat serum (Ivell and Barthold, unpublished observations).

To relate the in vitro INSL3-dependent gene expression results with potential INSL3-dependent gene expression during in vivo gubernacular development, we compared genes altered by INSL3 exposure in vitro and genes differentially expressed in male and female fetal gubernaculum in vivo. Although fetal males produce much higher levels of INSL3 compared to females [27], linking sexually dimorphic gubernaculum gene expression in vivo to INSL3 alone is confounded by the additional effects of androgen on gubernacular development [7, 9]. Nevertheless, a striking conservation of gene expression patterns was observed between gubernaculum INSL3 exposure in vitro and male and female gubernacula in vivo. Of genes stimulated at least twofold after INSL3 exposure in vitro and also compared between male and female gubernacula in vivo, approximately half (71/143) showed a similar response in both magnitude and direction of expression change. From these data, we conclude the following: 1) In vitro INSL3 exposure of gubernaculum explants recapitulates INSL3-dependent processes occurring in gubernaculum in vivo, and 2) many of the gene expression differences observed between male and female tissue in vivo are the result of higher INSL3 levels in males.

Although INSL3 increases cAMP production in gubernaculum through a G protein-dependent pathway, little else is known about the INSL3 signaling mechanism or its regulation. Our microarray expression data provide information about potential additional downstream INSL3 targets related to cAMP signaling. *Pnoc*, a cAMP-regulated gene [28], shows a rapid and robust response to INSL3 exposure in both male and female gubernaculum. *Crem*/*Icer* is another cAMP-inducible gene that represses cAMP-mediated signaling [24], and its expression was induced more than twofold by INSL3 exposure. INSL3 also regulated gubernaculum expression of phosphodiesterases, which can negatively regulate cellular cAMP levels and compartmentalize cAMP signaling processes to subcellular domains [29]. In vitro INSL3 exposure of the gubernaculum induced at least a twofold expression change of three phosphodiesterase mRNAs (*Pde10a*, *Pde8a*, and *Pde4*). In fact, *Pde10a* induction was among the highest observed, at more than 10-fold. Comparison of male and female gubernaculum gene expression corroborated this observation, because *Pde10a* expression was 13-fold higher in male compared to female GD 17 gubernaculum. These results support the hypothesis that increased phosphodiesterase, particularly *Pde10a*, and *Crem*/*Icer* expression in response to INSL3 exposure modulates INSL3-dependent signal transduction and gubernacular development.

Pathway analysis of gubernaculum INSL3-responsive genes suggested INSL3 mediates gubernacular development by inducing production of extracellular ligands and glycoproteins. Several IPA canonical pathways significantly over-represented in the INSL3 gene list were growth factor or morphogenetic signaling pathways, including HGF, WNT, and BMP signaling pathways. The mRNA expression of ligands driving these pathways was induced and included *Hgf* as well as a number of BMP family members (*Bmp1*, *Bmp2*, *Bmp3*, *Bmp5*, and *Bmp7*) and WNT family members (*Wnt2*, *Wnt4*, *Wnt5a*, *Wnt9a*, and *Wnt16*). Supporting a crucial role of both WNT and BMP signaling in gubernacular development are studies showing mutations in INSL3-regulated genes encoding secreted modulators of WNT and BMP signaling produce males with high intra-abdominal testes, including mouse mutations in *Bmp5* [30], the BMP antagonist *Nog* [31], the WNT pathway modulators *Sfrp1* and *Sfrp2* [32], and *Wnt5a* [32]. Cryptorchid phenotypes in WNT signaling pathway mutants appeared despite apparently normal testicular hormone production, and both WNT and BMP pathway mutants phenocopy genetic deletion of *Insl3* or *Rxfp2* [12–14]. DAVID bioinformatics analysis identified the GO cellular component term extracellular space (mainly comprised of secreted proteins) as significantly enriched by INSL3-responsive genes. In developing female mice transgenically overexpressing INSL3, gubernaculum enlargement similar to that in males and transabdominal migration of the ovary similar to that of the testis are observed. In our hands, the gene expression responses after INSL3 exposure of fetal male and female gubernaculum were similar. Collectively, these data suggest that an important downstream event of INSL3 during fetal gubernacular development is activation of Wnt and Bmp pathways via production of pathway ligands.

In addition to secreted factors and their signaling pathways, a major pathway identified by bioinformatics analysis of the microarray data was nervous system development. Using DAVID analysis of the INSL3-regulated gene lists, a number of related GO biological process annotations, such as neuron differentiation, generation of neurons, and neuron projection morphogenesis, were called significant. With both DAVID and IPA, the axonal guidance pathway was identified. Although these data suggest a role for INSL3 in neuronal development and/or function during the outgrowth phase of the fetal gubernaculum, INSL3 may have no direct effect on gene expression in nerve cells in our in vitro model of denervated gubernacula. Because RXFP2 is immunolocalized to gubernacular muscle cells [11], INSL3 may regulate trophic interactions between muscle cells and developing axons. Several genes with products that can regulate neuronal

development or function were induced at least 2-fold by INSL3, including *Wnt* family members [33], *Bmp* family members [33, 34], *Crlf1* [35, 36], *Gda* [37], *Nptx2* [38, 39], *Sema3g* [40], *Nfasc* [41, 42], and *Unc5d* [43]. The gene with the largest fold-change was *Pnoc* (34-fold), encoding the neuropeptide nociceptin, and the gene encoding a protease capable of prepronociceptin activation in vivo (*Pcsk2*) also was increased (6-fold) [44]. Nociceptin is regulated by cAMP, stimulates neuronal differentiation, and is expressed in and modulates release of calcitonin gene-related peptide (CGRP) in sensory neurons [28, 45, 46]. Interestingly, afferent CGRP release is postulated to stimulate motility of the gubernaculum during testis descent via receptors localized to muscle [47, 48], and sensory neuron number and CGRP content is altered in a congenitally cryptorchid rat strain [49].

In conclusion, novel microarray gene expression data and bioinformatics analyses describing molecular outcomes of INSL3 exposure in fetal gubernaculum are presented. Our results showed that INSL3 modulates the expression of approximately 900 genes with a concentration response similar to that of cAMP induction. Bioinformatics analysis suggests that a major biological outcome of INSL3 exposure includes transcriptional activation of neurodevelopmental genes. Based upon the known expression of the INSL3 receptor in gubernacular muscle, we hypothesize that INSL3 may contribute to neuromuscular signaling within the gubernaculum, possibly by secretion of muscle-derived neurotrophic factors. These data provide further insight regarding downstream pathways that contribute to gubernacular development and subsequent testis descent.

ACKNOWLEDGMENT

The authors thank Linda Pluta of The Hamner Institutes for Health Sciences for expert technical help in performing RNA labeling and microarray hybridization.

REFERENCES

1. Foresta C, Zuccarello D, Garolla A, Ferlin A. Role of hormones, genes, and environment in human cryptorchidism. Endocr Rev 2008; 29:560–580.
2. Barthold JS. Undescended testis: current theories of etiology. Curr Opin Urol 2008; 18:395–400.
3. Klonisch T, Fowler PA, Hombach-Klonisch S. Molecular and genetic regulation of testis descent and external genitalia development. Dev Biol 2004; 270:1–18.
4. Amann RP, Veeramachaneni DN. Cryptorchidism in common eutherian mammals. Reproduction 2007; 133:541–561.
5. Radhakrishnan J, Morikawa Y, Donahoe PK, Hendren WH. Observations on the gubernaculum during descent of the testis. Invest Urol 1979; 16: 365–368.
6. van der Schoot P. Towards a rational terminology in the study of the gubernaculum testis: arguments in support of the notion that the cremasteric sac should be considered the gubernaculum in postnatal rats and other mammals. J Anat 1996; 189(Pt 1):97–108.
7. Emmen JM, McLuskey A, Adham IM, Engel W, Grootegoed JA, Brinkmann AO. Hormonal control of gubernaculum development during testis descent: gubernaculum outgrowth in vitro requires both insulin-like factor and androgen. Endocrinology 2000; 141:4720–4727.
8. Fiegel HC, Rolle U, Metzger R, Geyer C, Till H, Kluth D. The testicular descent in the rat: a scanning electron microscopic study. Pediatr Surg Int 2010; 26:643–647.
9. Kubota Y, Temelcos C, Bathgate RA, Smith KJ, Scott D, Zhao C, Hutson JM. The role of insulin 3, testosterone, mullerian-inhibiting substance and relaxin in rat gubernacular growth. Mol Hum Reprod 2002; 8:900–905.
10. Bogatcheva NV, Truong A, Feng S, Engel W, Adham IM, Agoulnik AI. GREAT/LGR8 is the only receptor for insulin-like 3 peptide. Mol Endocrinol 2003; 17:2639–2646.
11. McKinnell C, Sharpe RM, Mahood K, Hallmark N, Scott H, Ivell R, Staub C, Jegou B, Haag F, Koch-Nolte F, Hartung S. Expression of insulin-like factor 3 protein in the rat testis during fetal and postnatal development and in relation to cryptorchidism induced by in utero exposure to di(n-butyl)phthalate. Endocrinology 2005; 146:4536–4544.
12. Zimmermann S, Steding G, Emmen JM, Brinkmann AO, Nayernia K, Holstein AF, Engel W, Adham IM. Targeted disruption of the Insl3 gene causes bilateral cryptorchidism. Mol Endocrinol 1999; 13:681–691.
13. Nef S, Parada LF. Cryptorchidism in mice mutant for Insl3. Nat Genet 1999; 22:295–299.
14. Tomiyama H, Hutson JM, Truong A, Agoulnik AI. Transabdominal testicular descent is disrupted in mice with deletion of insulin-like factor 3 receptor. J Pediatr Surg 2003; 38:1793–1798.
15. Koskimies P, Suvanto M, Nokkala E, Huhtaniemi IT, McLuskey A, Themmen AP, Poutanen M. Female mice carrying a ubiquitin promoter-Insl3 transgene have descended ovaries and inguinal hernias but normal fertility. Mol Cell Endocrinol 2003; 206:159–166.
16. Adham IM, Steding G, Thamm T, Bullesbach EE, Schwabe C, Paprotta I, Engel W. The overexpression of the insl3 in female mice causes descent of the ovaries. Mol Endocrinol 2002; 16:244–252.
17. Halls ML, van der Westhuizen ET, Bathgate RA, Summers RJ. Relaxin family peptide receptors—former orphans reunite with their parent ligands to activate multiple signaling pathways. Br J Pharmacol 2007; 150:677–691.
18. Kumagai J, Hsu SY, Matsumi H, Roh JS, Fu P, Wade JD, Bathgate RA, Hsueh AJ. INSL3/Leydig insulin-like peptide activates the LGR8 receptor important in testis descent. J Biol Chem 2002; 277:31283–31286.
19. Bogatcheva NV, Ferlin A, Feng S, Truong A, Gianesello L, Foresta C, Agoulnik AI. T222P mutation of the insulin-like 3 hormone receptor LGR8 is associated with testicular maldescent and hinders receptor expression on the cell surface membrane. Am J Physiol Endocrinol Metab 2007; 292:E138–E144.
20. van der Schoot P. Fetal testes control the prenatal growth and differentiation of the gubernacular cones in rabbits—a tribute to the late Professor Alfred Jost. Development 1993; 118:1327–1334.
21. Barthold JS, McCahan SM, Singh AV, Knudsen TB, Si X, Campion L, Akins RE. Altered expression of muscle- and cytoskeleton-related genes in a rat strain with inherited cryptorchidism. J Androl 2008; 29:352–366.
22. Huang da W, Sherman BT, Lempicki RA. Systematic and integrative analysis of large gene lists using DAVID bioinformatics resources. Nat Protoc 2009; 4:44–57.
23. Gonye GE, Chakravarthula P, Schwaber JS, Vadigepalli R. From promoter analysis to transcriptional regulatory network prediction using PAINT. Methods Mol Biol 2007; 408:49–68.
24. Borlikova G, Endo S. Inducible cAMP early repressor (ICER) and brain functions. Mol Neurobiol 2009; 40:73–86.
25. Liu H, Palmer D, Jimmo SL, Tilley DG, Dunkerley HA, Pang SC, Maurice DH. Expression of phosphodiesterase 4D (PDE4D) is regulated by both the cyclic AMP-dependent protein kinase and mitogen-activated protein kinase signaling pathways. A potential mechanism allowing for the coordinated regulation of PDE4D activity and expression in cells. J Biol Chem 2000; 275:26615–26624.
26. Anand-Ivell R, Heng K, Hafen B, Setchell B, Ivell R. Dynamics of INSL3 peptide expression in the rodent testis. Biol Reprod 2009; 81:480–487.
27. Anand-Ivell R, Ivell R, Driscoll D, Manson J. Insulin-like factor 3 levels in amniotic fluid of human male fetuses. Hum Reprod 2008; 23:1180–1186.
28. Zaveri NT, Waleh N, Toll L. Regulation of the prepronociceptin gene and its effect on neuronal differentiation. Gene 2006; 384:27–36.
29. Houslay MD, Baillie GS, Maurice DH. cAMP-specific phosphodiesterase-4 enzymes in the cardiovascular system: a molecular toolbox for generating compartmentalized cAMP signaling. Circ Res 2007; 100: 950–966.
30. Green MC. Mechanism of the pleiotropic effects of the short-ear mutant gene in the mouse. J Exp Zool 1968; 167:129–150.
31. Cook C, Vezina CM, Allgeier SH, Shaw A, Yu M, Peterson RE, Bushman W. Noggin is required for normal lobe patterning and ductal budding in the mouse prostate. Dev Biol 2007; 312:217–230.
32. Warr N, Siggers P, Bogani D, Brixey R, Pastorelli L, Yates L, Dean CH, Wells S, Satoh W, Shimono A, Greenfield A. Sfrp1 and Sfrp2 are required for normal male sexual development in mice. Dev Biol 2009; 326:273–284.
33. Charron F, Tessier-Lavigne M. The Hedgehog, TGF-beta/BMP and Wnt families of morphogens in axon guidance. Adv Exp Med Biol 2007; 621: 116–133.
34. Hodge LK, Klassen MP, Han BX, Yiu G, Hurrell J, Howell A, Rousseau G, Lemaigre F, Tessier-Lavigne M, Wang F. Retrograde BMP signaling regulates trigeminal sensory neuron identities and the formation of precise face maps. Neuron 2007; 55:572–586.
35. Forger NG, Prevette D, deLapeyriere O, de Bovis B, Wang S, Bartlett P, Oppenheim RW. Cardiotrophin-like cytokine/cytokine-like factor 1 is an

essential trophic factor for lumbar and facial motoneurons in vivo. J Neurosci 2003; 23:8854–8858.
36. Elson GC, Lelievre E, Guillet C, Chevalier S, Plun-Favreau H, Froger J, Suard I, de Coignac AB, Delneste Y, Bonnefoy JY, Gauchat JF, Gascan H. CLF associates with CLC to form a functional heteromeric ligand for the CNTF receptor complex. Nat Neurosci 2000; 3:867–872.
37. Chen H, Firestein BL. RhoA regulates dendrite branching in hippocampal neurons by decreasing cypin protein levels. J Neurosci 2007; 27:8378–8386.
38. O'Brien RJ, Xu D, Petralia RS, Steward O, Huganir RL, Worley P. Synaptic clustering of AMPA receptors by the extracellular immediate-early gene product Narp. Neuron 1999; 23:309–323.
39. Tsui CC, Copeland NG, Gilbert DJ, Jenkins NA, Barnes C, Worley PF. Narp, a novel member of the pentraxin family, promotes neurite outgrowth and is dynamically regulated by neuronal activity. J Neurosci 1996; 16: 2463–2478.
40. Taniguchi M, Masuda T, Fukaya M, Kataoka H, Mishina M, Yaginuma H, Watanabe M, Shimizu T. Identification and characterization of a novel member of murine semaphorin family. Genes Cells 2005; 10:785–792.
41. Ango F, di Cristo G, Higashiyama H, Bennett V, Wu P, Huang ZJ. Ankyrin-based subcellular gradient of neurofascin, an immunoglobulin family protein, directs GABAergic innervation at purkinje axon initial segment. Cell 2004; 119:257–272.
42. Volkmer H, Leuschner R, Zacharias U, Rathjen FG. Neurofascin induces neurites by heterophilic interactions with axonal NrCAM while NrCAM requires F11 on the axonal surface to extend neurites. J Cell Biol 1996; 135:1059–1069.
43. Moore SW, Tessier-Lavigne M, Kennedy TE. Netrins and their receptors. Adv Exp Med Biol 2007; 621:17–31.
44. Allen RG, Peng B, Pellegrino MJ, Miller ED, Grandy DK, Lundblad JR, Washburn CL, Pintar JE. Altered processing of pro-orphanin FQ/nociceptin and pro-opiomelanocortin-derived peptides in the brains of mice expressing defective prohormone convertase 2. J Neurosci 2001; 21: 5864–5870.
45. Capuano A, Curro D, Dello Russo C, Tringali G, Pozzoli G, Di Trapani G, Navarra P. Nociceptin (1–13)NH2 inhibits stimulated calcitonin-gene-related-peptide release from primary cultures of rat trigeminal ganglia neurones. Cephalalgia 2007; 27:868–876.
46. Pettersson LM, Sundler F, Danielsen N. Expression of orphanin FQ/nociceptin and its receptor in rat peripheral ganglia and spinal cord. Brain Res 2002; 945:266–275.
47. Momose Y, Griffiths AL, Hutson JM. Testicular descent. III. The neonatal mouse gubernaculum shows rhythmic contraction in organ culture in response to calcitonin gene-related peptide. Endocrinology 1992; 131: 2881–2884.
48. Yamanaka J, Metcalfe SA, Hutson JM, Mendelsohn FA. Testicular descent. II. Ontogeny and response to denervation of calcitonin gene-related peptide receptors in neonatal rat gubernaculum. Endocrinology 1993; 132:280–284.
49. Hrabovszky Z, Farmer PJ, Hutson JM. Undescended testis is accompanied by calcitonin gene related peptide accumulation within the sensory nucleus of the genitofemoral nerve in trans-scrotal rats. J Urol 2001; 165:1015–1018.